Trans. JWRI, Vol.24(1995), No.2

Measuring Methods of Three-Dimensional Residual Stresses with Aid of Distribution Function of Inherent Strains (Report 3) †

— Distributions of Residual Stresses and Inherent Strains in Fillet Welds —

Yukio UEDA* and Ning-Xu MA**

Abstract

In this paper, three dimensional residual stresses due to single pass and multipass fillet welding are analyzed by thermal elastic-plastic FEM. Then,, inherenet strain distributions produced in fillet welds are described by series function. Based on the results of series function descriptions for inherent strains, a simplified distribution pattern for inherent strains is derived and described by a simple function with a very small number of unknown parameters. If these unknown parameters are to be determined by experiments, the required measurements will be greatly reduced.

KEY WORDS: (Residual Stresses) (Inherent Strains) (Distribution Functions) (Fillet Welds) (FEM)

1. Introduction

It is well known that the welding stresses in fillet welds, especially the local distribution near fillet weld toes and through the plate thickness are directly related to the cracking[1-2] during welding and fatigue cracking[3] during performance. The measurement for the detail distributions of residual stresses using strain gauges becomes very difficult because of the limitations of the the strain gauge size and cutting process. To solve these problems, the layer-removal method [4] and slit cutting method[5-6] have been developed. However, using these methods, some limited residual stress components distributed at special positions or sections where metal is removed can be estimated. In this paper, attention is paid to inherent strain [7-10] as a source of residual stresses. Then, the distribution characteristics of inherent strain in fillet welded joints are investigated. Furthermore, the inherent strain distribution functions are derived. With the aid of distribution functions, three dimensionl residual stresses including local distributions can be estimated using a very small number of measured data.

To investigate the inherent strain distributions in fillet welds, the welding residual stresses are firstly computed by thermal elastic-plastic FEM. Using the computed residual stresses, the inherent strains are estimated, and then their distribitions are described as functions. The accuracy of the distribution functions for inherent strains is verified by comparing the reproduced residual stresses using inherent strains with the computed ones using thermal elastic-plastic FEM.

2. Modelling of Fillet Welds

2.1 Analyzing Model

The analyzing model is assumed to be an infinitely long T-type fillet weld. The transverse section of the T-type fillet weld is shown in **Fig.** 1. The width and thickness of flange are denoted by $2B_W$ and H_F respectively, those of web are denoted by B_W and $2H_W$ respectively.

As shown in **Figs** .1 (a) and (b), there are two kinds of fillet welds which are called partial penetration and full penetration welds. For the partial penetration fillet welds, there exists a gap between flange and web. The length of the gap is denoted by 2g. When the welding heat input increases, the penetration will become deep and the gap

† Received on Nov. 24, 1995
* Professor
** Research Associate

Transactions of JWRI is published by Welding Research Institute of Osaka University, Ibaraki, Osaka 567, Japan.

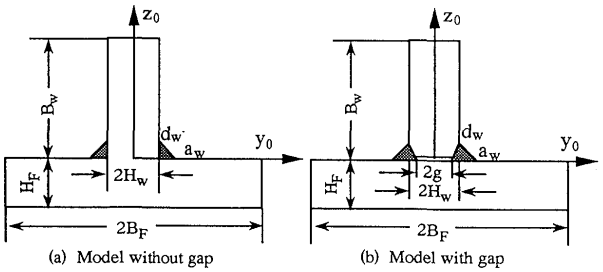

Fig. 1 Models of fillet welds

length will become small. The full penetration fillet weld is only a special case when the gap length 2g is zero. Therefore, the partial penetration fillet weld is considered as a general analyzing model in this paper.

To investigate the effect of gap on residual stresses and inherent strains in fillet welds, the partial penetration model without gap is also assumed in the analysis.

Firstly, the residual stresses and inherent strains in the model with very thick flange and web are simulated by thermal elastic-plastic FEM. Then those in relatively thin plate and multipass fillet welds are discussed.

2.2 Analyzing Conditions

In actual welding, the welding torch is moving. In this analysis, the two welds at the left and right sides of web are assumed to be welded simultaneously. In the partial penetration welding, the heat transfer between two surfaces of gap is neglected. The material used in the analysis is assumed to be mild steel. The physical and mechanical properties of the steel used in the analysis are shown in the **Figs.** 2 and 3, respectively. As shown in **Fig.** 3, when the temperature is higher than Tm, the yield stress and Young's modulus of the material become very small. This temperature is called mechanical melting point. It is about 700°C for mild steel. The zone where the maximum temperature in the thermal cycles is higher than Tm is called HAZ in this paper.

For a very long fillet weld, it can be assumed that the stress and strain distribute uniformly in the welding direction except at the two ends of the weld line. The longitudinal deformation strain ε_x distributed in the transverse section (y-z plane) can be assumed to be a linear function of y and z coordinates during welding process and after welding. i.e.,

$$\varepsilon_x=a_0+a_1y+a_2z \quad (1)$$

This kind of deformation is called generalized plane strain. Using this deformation condition, three dimensional residual stresses and inherent strains can be simulated by taking the transverse section with unit thickness as an analyzing model.

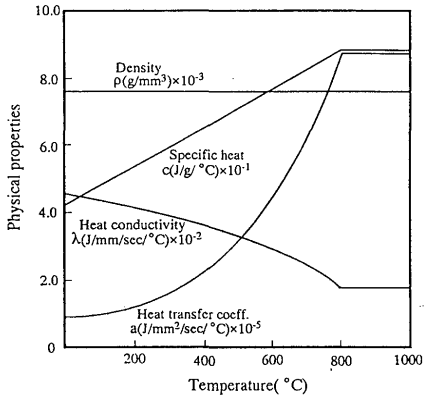

Fig. 2 Physical properties of mild steel used in analysis

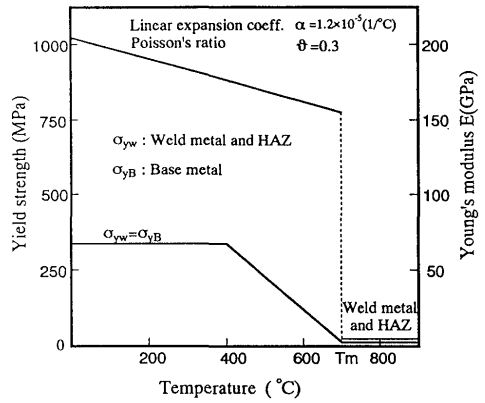

Fig. 3 Mechanical properties of mild steel used in analysis

3. Distributions of Residual Stresses in Fillet Welds

3.1 Distributions of Temperature

When the equivalent heat input Q=1500 (J/mm.Sec) for unit weld length is applied to the T-type fillet weld with the sizes B_F=250 mm, H_F=30 mm, B_w=220 mm, H_w=30 mm, the distributions of the maximum temperature reached in the thermal cycles on the transverse section computed by thermal conduction FEM are shown in **Fig.** 4 and **Fig.** 5 in the non gap fillet model and gap fillet model, respectively. The residual plastic strain zones in the fillet welds computed by thermal elastic-plastic FEM are also shown in these Figures.

It can be concluded from **Figs.** 4 and 5 that the shape of the maximum temperature contours consist of three partial ellipses in flange and web whose origin is the center of the fillet welded metal. The similar shape of plastic strain zone can be also observed in these Figures. At the two sides of the gap between flange and web, the temperature and plastic strain have discontinuous distributions.

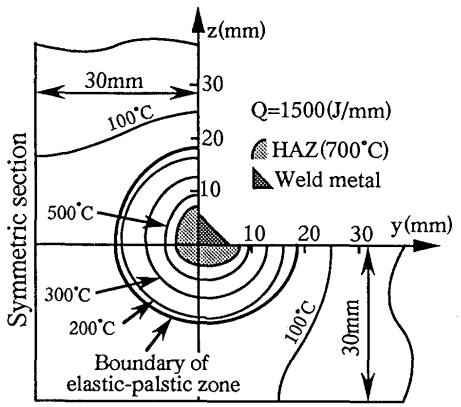

Fig. 4 Distributions of max. temperature in thermal cycles and plastic deformation zone in non gap fillet model

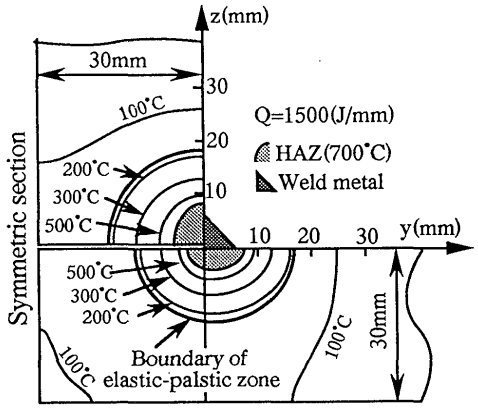

Fig. 5 Distributions of max. temperature in thermal cycles and plastic deformation zone in gap fillet model

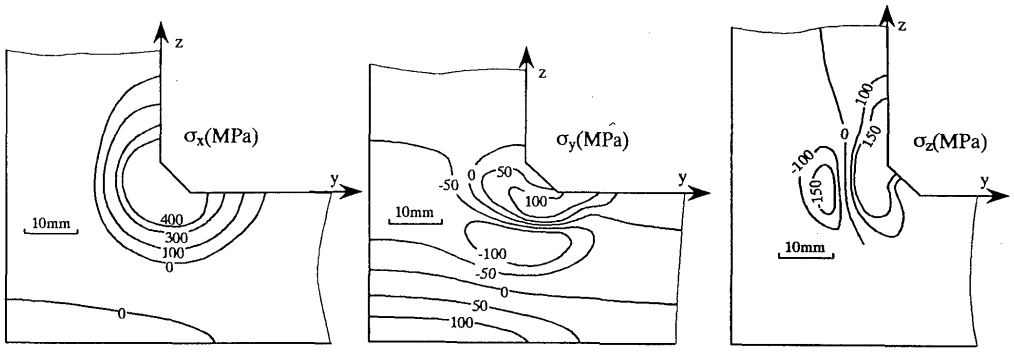

(a) Distribution of residual stress σ_x (b) Distribution of residual stress σ_y (c) Distribution of residual stress σ_z

Fig. 6 Distributions of residual stresses in non gap fillet model

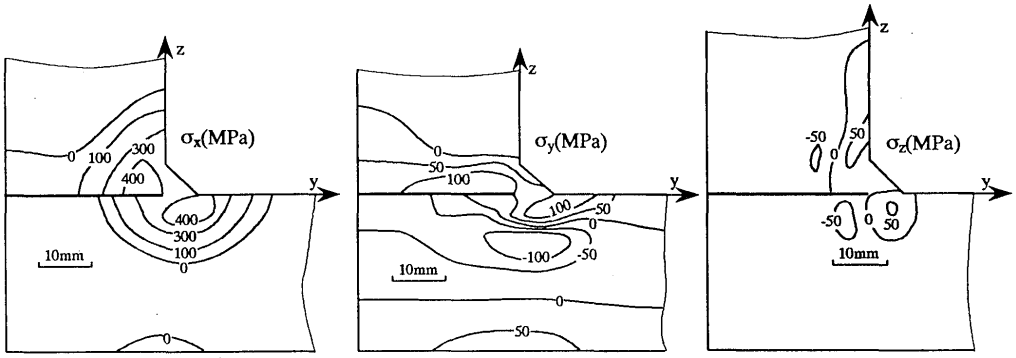

(a) Distribution of residual stress σ_x (b) Distribution of residual stress σ_y (c) Distribution of residual stress σ_z

Fig. 7 Distributions of residual stresses in gap fillet model

3.2 Distribution of Residual Stresses

For the non gap fillet weld model is used in the FEM analysis, the computed three dimensional residual stress distributions are shown in **Fig.** 6. In the zone in/near welded metal, tensile residual stresses σ_X, σ_Y and σ_Z can be observed. The residual stress σ_X is larger than σ_Y and σ_Z. Near the fillet welded toes, very large tensile stresses σ_Y and σ_Z are produced.

When the gap between flange and web are considered in the FEM analysis, the computed residual stress distributions are shown in **Fig.** 7. The local residual stress distributions near the gap and in the web show some large changes compared with those in the non gap fillet model. If attention is only paid to the overall distributions or the residual stresses in flange, or near the fillet toes, onlys mall changes can be observed. In this case, the effect of gap can be neglected in the FEM modelling.

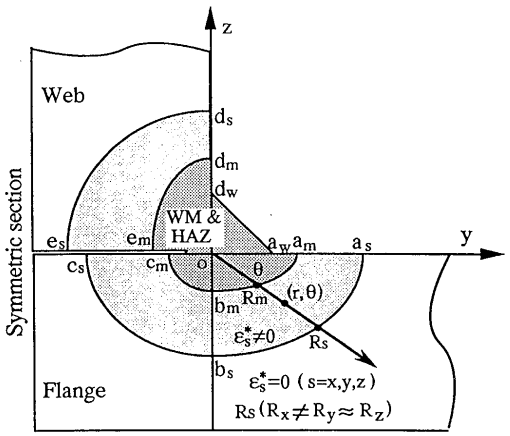

Fig. 8 Distribution zones of inherent strains in fillet welds

4 Distributions of Inherent Strains in Fillet Welds

4.1 Inherent Strain Components and Their Distribution Zones

It can be assumed that only the three normal inherent strain components ε^*_x, ε^*_y and ε^*_z exist in a very long fillet weld, which are the component of welding direction (x), transverse direction of flange (y) and transverse direction of web (z). To simplify the expression, these components are denoted by ε^*_s, the subscript 's' is used to present x, y and z, respectively.

According to the maximum temperature contours and plastic strain zone shown in **Fig.** 4 and **Fig.** 5, the distribution zone of inherent strains can be simplified as three partial ellipses (oa_sb_s, ob_sc_s, oe_sd_s) and the fillet weld metal (oa_wd_w) shown in **Fig.** 8. The sizes of inherent strain zones can be different with the inherent strain components. As reported in previous paper[8], the distribution zone of ε^*_x is larger than those of ε^*_y and ε^*_z corresponding to the magnitude of their stress components. The sizes of distribution zones of inherent strain components ε^*_y and ε^*_z within the transverse section can be considered to be the same.

When the shape of inherent strain zones is described by three partial ellipses, their sizes can be expressed by a_s, b_s, c_s, e_s, d_s (s=x, y, z) shown in **Fig.** 8. The sizes (a_x, b_x, c_x, e_x, d_x) of inherent strain ε^*_x can be estimated from the distributions of residual stress σ_x in y and z directions shown in **Fig.** 9. For instance, a_x can be determined from the bending point in the compressive side of stress σ_x. The sizes ($a_y=a_z$, $b_y=b_z$, $c_y=c_z$, $e_y=e_z$, $d_y=d_z$) of inherent strain ε^*_y and ε^*_z can be estimated from the distributions of residual stresses σ_y and σ_z in y and z directions. For instance, a_y can be determined from the point on the flange surface where the maximum tensile stress σ_y is produced. b_y corresponds to the point

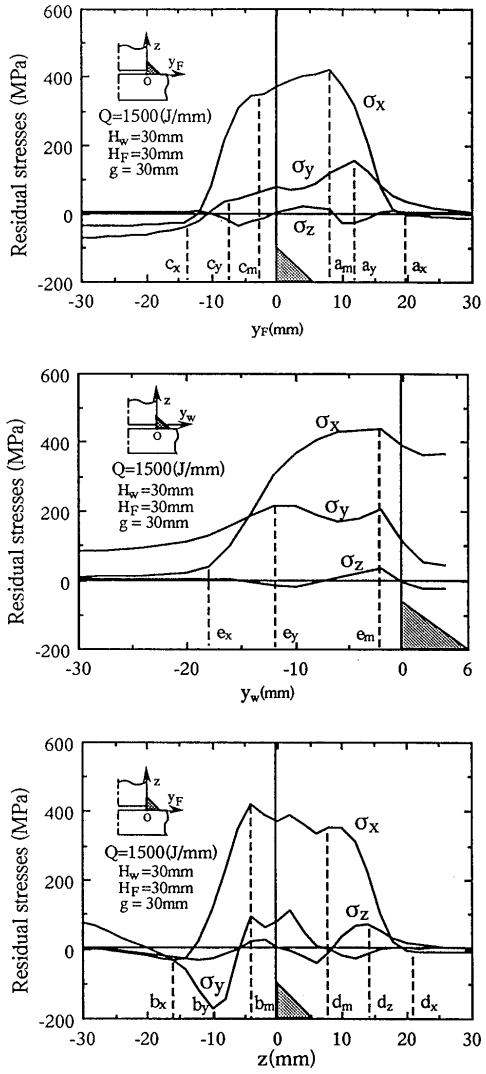

Fig. 9 Determination of the sizes of inherent strain zones from stress distributions in y and z directions

of the maximum compressive stress σ_y distributed through the thickness of flange. When the gap between flange and web is neglected, the $c_s=e_s$ (s=x, y, z).

In **Fig.** 8, the shape of the HAZ is also assumed to be composed of three partial ellipses and their sizes are expressed by (a_m, b_m, c_m, e_m, d_m). (a_m, b_m, c_m, e_m, d_m) can also be determined from the stress distributions in y and z directions[8-9] shown in **Fig.** 9

When plate thickness is small compared with the welding heat input, the size of b_x, c_x and e_x of inherent strain ε^*_x distributed through the thickness become larger than the plate thickness. However, the zone of effective inherent strain components ε^*_y and ε^*_z within a transverse section can be considered to be still smaller than the plate thickness because the linear distribution of inherent strain ε^*_y and ε^*_z through thickness does not produce residual stresses.

4.2 Series Function Description for Inherent Strain Distributions

In order to describe the inherent strain distributions by functions, the dimensionless form (ξ_s, ω) of a polar coordinate system (r, θ) is defined by the following equation:

$$\xi_s = \frac{r}{R_s}, \quad \omega = \frac{\theta}{2\pi}, \quad (s=x, y, z) \tag{2}$$

Where R_s is the radius of inherent strain zones which vary with θ. When θ is in the range of 270°-360°, the R_s is supposed to be the radius of ellipse (oa_sd_s)

The range of ξ_s is from 0 to 1. ξ_s=0 and ξ_s=1 indicate the center of the ellipse and boundary curve of inherent strain zones, respectively. ω=0, ω=0.25, ω=0.5 and ω=0.75 indicate the positive y axis (θ=0), positive z axis ($\theta=\pi/2$), negative y axis ($\theta=\pi$) and negative z axis ($\theta=3\pi/2$), respectively. When dimensionless polar coordinates (ξ_s, ω) are employed here, inherent strain distribution for each component ε^*_s (s=x, y, z) can be described by the following general series function:

$$\varepsilon^*_s(x,y,z)=\sum_{i=1}^{M}\sum_{j=1}^{N}A^*_{sij}\, f_{si}(\xi_s)\, g_{sj}(\omega), \quad (s=x, y, z) \tag{3}$$

For $f_{si}(\xi_s)$ and $g_{sj}(\omega)$, many types of functions can be considered, such as power functions, exponential functions and trigonometric functions. In this paper, very simple power functions are used, and inherent strain distributions are expressed by:

$$\varepsilon^*_s(x,y,z)=\sum_{i=1}^{M}\sum_{j=1}^{N}A^*_{sij}\,(1-\xi_s)^i\,\omega^{(j-1)}, \quad (s=x, y, z) \tag{4}$$

The values of inherent strain given by Eq.(4) are zero at the boundary curve (ξ_s=1) of inherent strain zones. When M=N=1, an uniform distribution in the θ direction can be described

When inherent strain is described by a series function (4), its distributions will be determined only by the coefficients included in the function. The elastic response relationship between coefficient vector $\{A^*\}_p$ and elastic strain $\{\varepsilon^e\}$ at m number of arbitrary positions can be expressed by:

$$[G]_{mp}\{A^*\}_p = \{\varepsilon^e\}_m \tag{5}$$

where $[G]_{mp}$ is the elastic response matrix between $\{A^*\}_p$ and $\{\varepsilon^e\}$. The component G_{ij} of matrix $[G]_{mp}$ is equal to the value of the i-th elastic strain ε^e_i, generated by an assumed inherent strain distribution corresponding to the unit coefficient for j-th order (A^*_j=1) and zero for coefficients A^*_k(if k≠j) in $\{A^*\}_p$[8].

When these coefficients are estimated by Eq. (5) using a small number of elastic strains, the elastic strain $\{\varepsilon^e\}$ and residual stress $\{\sigma\}$ at all positions can be computed by the following equation:

$$\{\varepsilon^e\}=[G]\{A^*\}_p \qquad \{\sigma\}=[D]\{\varepsilon^e\} \tag{6}$$

where [D] is the strain-stress matrix composed of Young's modulus E and Poisson's ratio υ.

4.3 Accuracy of Series function description for inherent strain distributions

The accuracy of the series function description for inherent strains can be evaluated by the error in residual stresses reproduced by inherent strains. The error in the reproduced residual stresses is shown by following equation:

$$E_r = \sqrt{\sum_{i=1}^{m}(\sigma_i^m - \sigma_i^e)^2} \Big/ \sqrt{\sum_{i=1}^{m}(\sigma_i^m)^2} \tag{7}$$

where σ_i^m is the residual stress directly measured or computed by thermal elastic plastic FEM, σ_i^e is the residual stress reproduced by inherent strain whose distributions are described by functions, and m is the total number of residual stresses directly measured or computed by thermal elastic plastic FEM analysis

E_r is called the normalized root mean square error[11]. It can express the total error of m components of measured residual stresses. Therefore, it is called total error. Besides the total error, to evaluate the accuracy of local residual stresses, the ratio of maximum absolute error ($\max|\sigma_i^m-\sigma_i^e|$) of reproduced residual stresses to the yield stress (σ_{yw}) of welded metal is introduced as the local maximum error e_r, i.e.

$$e_r = \max|\sigma_i^m-\sigma_i^e|/\sigma_{yw}, \quad (i=1, 2,...,m) \tag{8}$$

When inherent strain distributions are expressed by the series function, the accuracy is governed by the order M and N of series function. The effects of M and N, or the total number p_s (=M×N) of unknown coefficients for each inherent strain component ε^*_s (s=x, y, z) on the errors Er and e_r of reproduced residual stresses, are shown by **Fig. 10**.

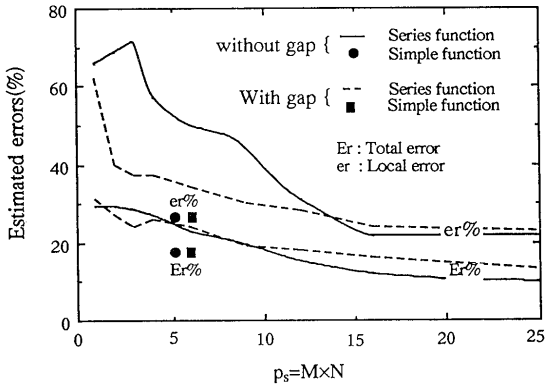

Fig. 10 Accuracy of function description for inherent strains in fillet welds

By increasing the order M and N of the series function, or by increasing the total number p_S(=M×N) of unknown coefficients, the total error E_r and local error e_r decrease. In actual measurements, according to the expected accuracy, M and N of the series function, or measuring points corresponding to the total number p_S(=M×N) of unknown coefficients, can be freely selected. As shown in **Fig.** 10, when M and N are more than 4, or the total number p_s of unknown coefficients is more than 16 in both gap fillet model and non gap fillet models, the change of errors becomes smaller and practically reasonable accuracy can be obtained.

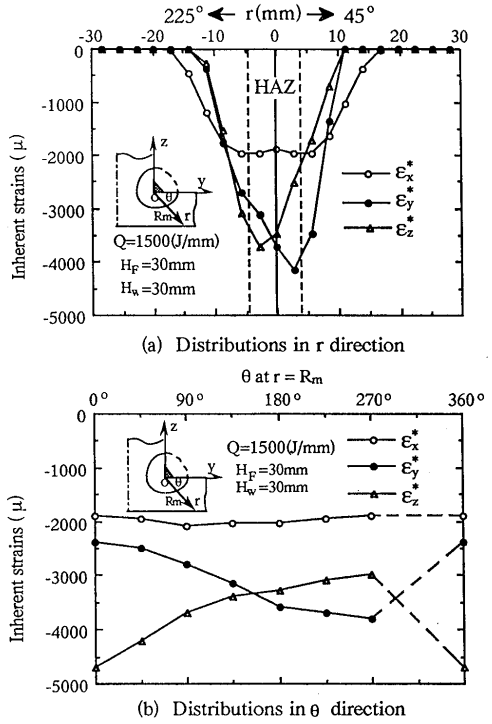

(a) Distributions in r direction

(b) Distributions in θ direction

Fig. 11 Estimated inherent strain distributions in r and θ directions using sereios function (non gap fillet model)

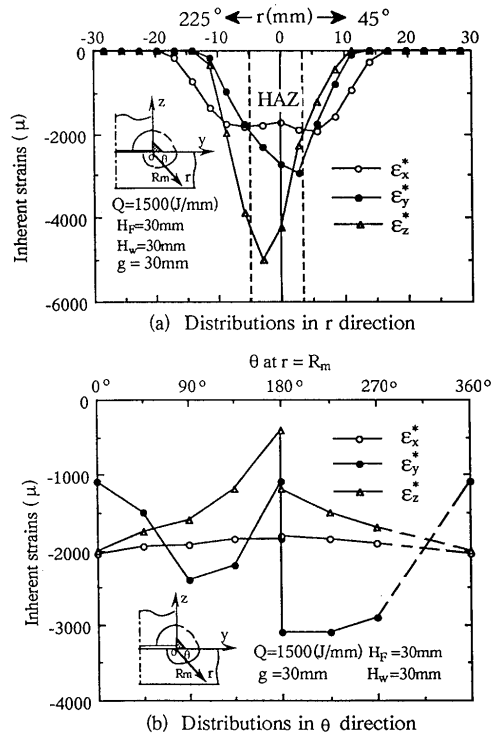

(a) Distributions in r direction

(b) Distributions in θ direction

Fig. 12 Estimated inherent strain distributions in r and θ directions using sereios function (gap fillet model)

In the non gap fillet model, when M=N=4 for series function (4), the estimated inherent strain distributions in the r direction (at θ=45° and θ=225°) and θ direction of HAZ boundary curve ($r=R_m$) are shown in **Fig.** 11. In the r direction, the inherent strain distributions have trapezoidal shape. In the θ direction of the HAZ boundary curve, inherent strains distribute approximately linearly in the range of 0°-90°, 90°-180°, 180°-270° and 270°-360°, respectively. In the **Fig.** 11, the broken lines indicate the inherent strains between the 270°-360° in the θ direction of supposed HAZ boundary (a_m-d_m).

The inherent strain distributions in the gap fillet welds are shown in **Fig.** 12. At the two sides of the gap, a sudden change of inherent strains can be observed. Except for the discontinuous distributions at the gap position, the distribution patterns of inherent strains for these two models are similar.

4.4 Simple Function Description for Inherent Strain Distributions

When the inherent strain distributions are described by series function, the accuracy is related to the order of M and N of the series function. To obtain high accuracy, a large order of M and N have to be selected. This means the unknown parameters will increase. To solve this problem, a simplified distributon pattern of inherent strains is proposed as shown in **Fig.** 13. Inherent strains in this pattern change linearly in r direction within the weld metal and HAZ, and decrease gradually out of the HAZ and become zero outside inherent strain zones. This inherent strain distribution pattern can be described by a simple function shown in following equation :

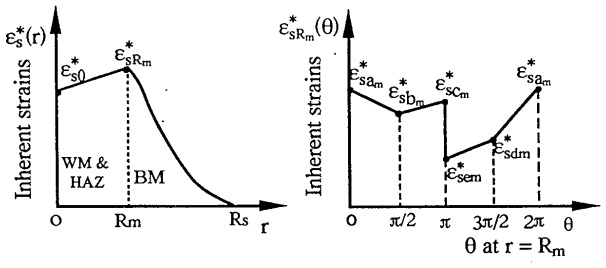

Fig. 13 Simplified distribution pattern of inherent strains in fillet welds

$$\varepsilon^*_s(r) = \begin{cases} (1-\frac{r}{R_m})\,\varepsilon^*_{s0} + \frac{r}{R_m}\varepsilon^*_{sRm}(\theta) & (0 \le r \le R_m) \\ \exp\left(\frac{-3(r-R_m)^2}{(R_s-R_m)^2}\right)\varepsilon^*_{sRm}(\theta) & (R_m \le r \le R_s) \end{cases}$$

$$\varepsilon^*_{sRm}(\theta) = \begin{cases} (1-\frac{\theta}{\pi/2})\,\varepsilon^*_{sam} + \frac{\theta}{\pi/2}\varepsilon^*_{sbm} & (0 \le \theta \le \pi/2) \\ (1-\frac{\theta-\pi/2}{\pi/2})\,\varepsilon^*_{sbm} + \frac{\theta-\pi/2}{\pi/2}\varepsilon^*_{scm} & (\pi/2 \le \theta \le \pi) \\ (1-\frac{\theta-\pi}{\pi/2})\,\varepsilon^*_{scm} + \frac{\theta-\pi}{\pi/2}\varepsilon^*_{sdm} & (\pi \le \theta \le 3\pi/2\pi) \\ (1-\frac{\theta-2\pi/2}{\pi/2})\,\varepsilon^*_{sdm} + \frac{\theta-3\pi/2}{\pi/2}\varepsilon^*_{sdm} & (3\pi/2 \le \theta \le 2\pi) \end{cases}$$

$$(s = x, y, z) \qquad (9)$$

Here, a linear function is used to express the distribution in the r direction within the HAZ and an exponential function is used for the distribution in the r direction out of the HAZ. The inherent strains at the HAZ boundary line $\varepsilon^*_{s\,Rm}$ (s=x, y, z) can be calculated by linear functions in the range of θ = 0°-90°, 90°-180°, 180°-270° and 270°-360°, respectively. In the region of θ = 270°-360°, R_m is the radius of the supposed ellipse (oa_md_m).

In the simple function (9), there are two kinds of unknown parameters which are, the sizes of inherent strain zones and the magnitude of inherent strains at 6 points (O, a_m, b_m, c_m, e_m and d_m) which are denoted by $[A^*]_p$ below :

$$\{A^*\}_p = \{\varepsilon^*_{sO}, \varepsilon^*_{sam}, \varepsilon^*_{sbm}, \varepsilon^*_{scm}, \varepsilon^*_{sem}, \varepsilon^*_{sdm}\}^T \quad (s=x, y, z) \qquad (10)$$

In the non gap fillet model, both the sizes of inherent strain distribution zones and the magnitude of the inherent strains at the two sides of gap will become the same.

For inherent strain component ε^*_x, the uniform distribution within the HAZ can be assumed according to the results of the series function description of inherent strains shown in **Figs.** 11 and 12. i.e.

$$\varepsilon^*_{xO} = \varepsilon^*_{xam} = \varepsilon^*_{xbm} = \varepsilon^*_{xcm} = \varepsilon^*_{xem} = \varepsilon^*_{xdm} \qquad (11)$$

When the simple function for inherent strain distributions is employed, the total error E_r and local maximum error e_r of reproduced residual stresses in both the gap fillet model and non gap fillet model, are shown in **Fig.**10. Compared with the series function for inherent strains, the simple function has fewer unknown parameters and almost the same accuracy.

5 Application of Inherent Strain Distribution Functions to Multipass Fillet Weld

Fig.14 shows the multipass fillet weld used in this analysis. It is a partial penetration, 5 passes and 3 layers fillet weld. The thickness of flange and web are H_F=20 mm and H_w=10 mm. The fillet sizes are a_w=d_w=14 mm. It is assumed that the new welding pass starts when the temperature induced by provious welding pass cools

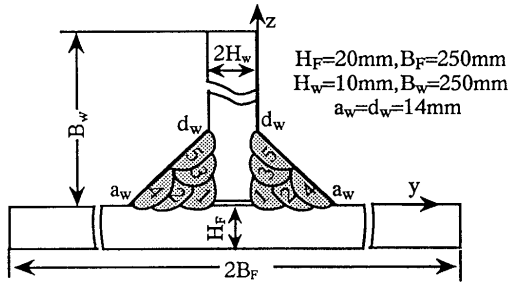

Fig. 14 A multipass T-type fillet weld to be analyzed

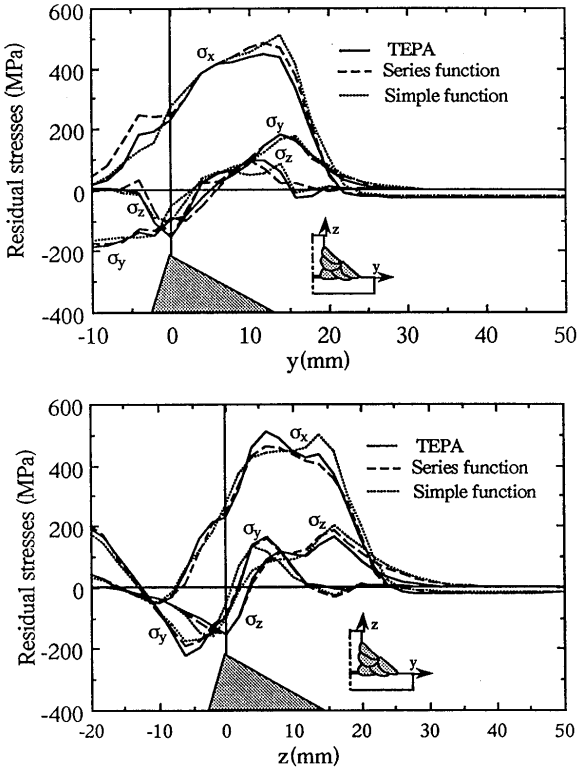

Fig. 15 Residual stresses estimated by Thermal-Elastic-Plastic-Analysis (TEPA) and Inherent-Strain-Elastic-Analysis (ISEA)

down, and that welding is conducted simultaneously at both sides of web. The equivalent heat input per unit weld length is 630, 630, 630, 720 and 720 (J/mm.Sec) for each of the 5 passes. As the analyzing sequence, firstly the residual stresses due to multipass welding are simulated by FEM, then the residual stresses are reproduced by inherent strains whose distributions are expressed by series function and simple function, respectively.

The residual stress distributions in y and z directions of multipass fillet weld computed by Thermal Elastic Plastic Analysis (TEPA) are shown by the solid lines in **Fig.** 15. The overall distributions are similar to those in single pass welding and large transverse tensile residual

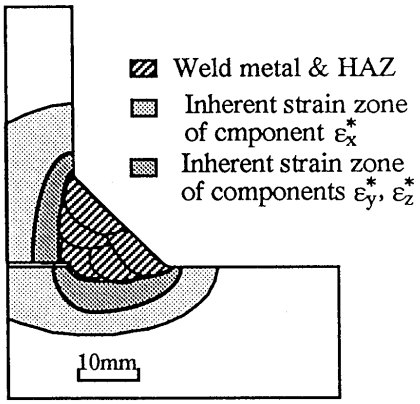

Fig.16 Inherent strain zones in a multipass fillet weld

stresses are produced on the surface near the multipass fillet weld toes.

From the computed residual stress distributions by TEPA, the distribution zones for inherent strain components ε^*_x, ε^*_y and ε^*_z are estimated as shown **Fig.** 16. In this case, the inherent strain ε^*_x distributes through all the thickness of the web. The sizes of the HAZ are also shown in the **Fig.** 16.

When the inherent strain zones are determined, inherent strain distributions in these zones can be easily estimated with the aid of the series function and simple function described previously. The residual stresses reproduced by estimated inherent strains using series function with M=N=4 and simple function, are shown in **Fig.**15 by the broken lines and point lines, respectively. From the **Fig.** 15, it can be observed that the both functions can reproduce the welding residual stresses with very good accuracy compared with the results of TEPA.

6. Conclusions

(1) Residual stress distributions in both gap fillet weld and non gap fillet weld are clarified by thermal elastic plastic FEM. The gap has some effects on the local transverse residual stresses near the gap and in the web, but it has very small effect on the residual stresses in the flange.

(2) Inherent strain zones can be simplified by three partial ellipses and fillet weld metal. The sizes of inherent strain zones at the two sides of the gap are different.

(3) Series functions and simple functions for inherent strain distributions are proposed. The residual stresses reproduced using these functions show a very good accuracy compared with the results of thermal elastic plastic FEM.

(4) The distribution functions for inherent strains are also valuable for multipass fillet welds.

References

1) Y. Ueda, K. Fukuda and K. Nakacho : Study on Type of Cracking of Fillet Weld Based on Residual Stresses Calculated by FEM, Journal of Japan Welding Socety, Vol.44 (1975) N0.3, pp. 74-81

2) Y. Ueda, K. Fukuda and N. Chiba : Dynamical Characteristics of Welding Cracking in Multipass Welded Corner Joint, Journal of Japan Welding Socety, Vol.48 (1979) N0.1, pp. 34-39

3) K. Ohji : Futigue Crack Propagation in Residual Stress Field, Third Int. Conf. on Residual Stresses, Tokushima, Japan, 23-26 July, 1991, Residual Stresses III, Ed. H. Fujiwana et al, Elsevier Applied Science, pp. 447-456

4) Y. Ueda, H. Murakawa and N.X. Ma : Measurement of Residual Stresses in Explosively Clad Steel and A Method of Residual Stress Reduction, JWRI, Vol.23, No.2(1994), pp.249-255

5) D. Ritchie, R.H. Reggatt : The Measurement of The Distribution of Residual Stresses through The Thickness of A Welded Joint, Stain, May, 1987

6) W. Cheng I. Finnie : The Crack Compliance Method for Residual Stress Measurement, Welding in The World, 5/6, Sept. 1990

7) Y. Ueda, K. Fukuda : New Measuring Method of Three-dimensional Residual Stresses Based on Theory of Inherent Strain, J. Soc. Naval Arch. of Japan, Vol.145(1979), pp.203-211(in Japanese). Also Trans. JWRI, Vol.8, No.2(1979), pp.249-256.

8) Y. Ueda and N.X. Ma : A Function Method for Inherent Strain Distributions, Quartely Journal of Japan Welding Society, Vol.11 (1993) NO.1, PP.189-195, Also JWRI, Vol.23, No.1(1994), pp.71-78

9) Y. Ueda and N.X. Ma : TLyLz-Method and T-Method for Measurement of 3-Dimensional Residual Stresses in Bead-on-Plate Welding, Quartely Journal of Japan Welding Society, Vol.11 (1993) NO.4, PP.555-562, Also JWRI, Vol.23, No.2(1994), pp.239-247

10) Y. Ueda, M.G. Yuan : A Predicting Method of Welding Residual Stress Using Source of Residual Stress (Report 1), Vol.6, No.1(1988) (in Japanese). Also Trans. JWRI, Vol.18, No.1(1989), pp.135-141.

11) J.S. Bendat and A.G.Piersol : RANDOM DATA of Analysis and Measurement Procedures, Copyright 1971, by John Wiley & Sons. Inc. Translated in Japanese by Tokumaru hidekatsu, 1973.